Controlledin situnanoscale enhancement of gold nanowire arrays with plasmonics

MacKenzie, R ; Fraschina, C ; Sannomiya, T ; Vörös, J

DOI: https://doi.org/10.1088/0957-4484/22/5/055203

Controlled *in situ* nanoscale enhancement of gold nanowire arrays with plasmonics

2011 Nanotechnology 22 055203

(http://iopscience.iop.org/0957-4484/22/5/055203)

Nanotechnology **22** (2011) 055203 (8pp) doi:10.1088/0957-4484/22/5/055203

Controlled *in situ* nanoscale enhancement of gold nanowire arrays with plasmonics

Robert MacKenzie, Corrado Fraschina, Takumi Sannomiya and Janos Vörös

Laboratory of Biosensors & Bioelectronics, ETH Zurich, Gloriastrasse 35, 8092 Zurich, Switzerland

E-mail: janos.voros@biomed.ee.ethz.ch

Received 12 October 2010
Published 22 December 2010
Online at stacks.iop.org/Nano/22/055203

Abstract

The controlled *in situ* growth of ordered gold nanoparticles and nanowire arrays has been studied by optically tracking changes in the local surface plasmon resonance (LSPR) spectrum. A spectrometer and custom-programmed analysis software track changes in the LSPR spectrum. The peak position, peak height (i.e. extinction intensity) and peak width (e.g. radius of curvature) were tracked over time to quantify the dynamic growth of gold as soon as the system was exposed to a commercial gold enhancement solution. This enables the controlled dynamic growth of nano-objects without the necessity of characterizing the growth and aggregation kinetics of the gold enhancement solution. The result was the successful enhancement of their electrically conductive and plasmonic properties, as well as the controlled growth and transformation of line-patterned nanoparticles into conductive particle-based nanowires.

S Online supplementary data available from stacks.iop.org/Nano/22/055203/mmedia

(Some figures in this article are in colour only in the electronic version)

1. Introduction

Existing nano-patterning techniques, such as e-beam lithography (EBL) [8, 25], focused ion-beam lithography (FIBL) [24], dip-pen lithography [7, 26] and extreme ultraviolet light interference lithography (EUV-IL) [2] provide controllable and reliable fabrication of nano-patterned surfaces and nanostructures. However, once created the question arises of how to further extend these methods, specifically adapt or even repair these nanostructures directly on the nanoscale. In other words, if nanostructures are able to be fabricated through conventional methods with a separation of e.g. 10 nm, could an extension of this method reliably reduce the separation to sub 10 nm dimensions? Intuitively one would like to visualize such a process and see what is dynamically changing, such as with electron microscopy as the typical tool to directly visualize nanoscale objects. However, the requirement of conventional electron microscopy of only being able to visualize entirely conductive or conductively coated substrates is a limitation. Therefore, there is still a strong need to develop other techniques that enable the fast, reliable and dynamic optimization or enhancement of pre-existing nanostructures directly on the nanoscale. Here then the rhetorical question: is it possible to controllably and consciously change nanostructures and/or precisely tailor the separation between nano-objects on a surface without directly seeing them?

For the specific case of gold nano-objects this work proposes such a novel method. Although not shown in this work, the chemistry and method would also be extendable to silver nano-objects. This would be useful in several areas, such as nanogap sensing and nanoelectronics. Localized surface plasmon resonance (LSPR) is another specific example, in which the shape, profile and inter-object spacing on the nanoscale are critical parameters for the optical performance of the system. This performance is often characterized by such parameters as the nanostructure's LSPR frequency (or frequencies), intensity and field decay length. On an application level nanoparticles and nanowires, in combination with LSPR, have proven to be effective nanostructures for the creation of novel electrochemical and biosensing systems [13, 14, 17, 18, 20]. Additional practical LSPR-based applications are emerging, such as the technique of using optically coupled plasmonic particles for strain mapping,

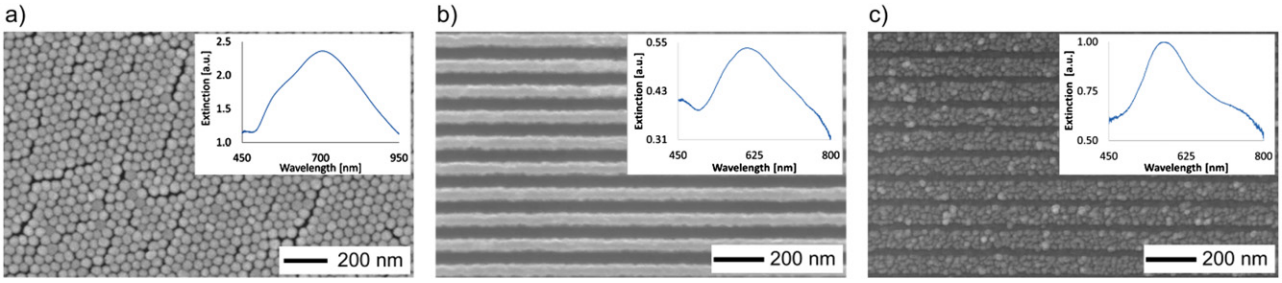

Figure 1. (a) A monolayer of 50 nm gold nanoparticles in a hexagonal arrangement; (b) evaporated gold nanowires; (c) particle-based nanolines from EUV-IL assisted self-assembled 5 nm gold nanoparticles before their enhancement into conductive nanowires. The periodicity of the nanoline and nanowire arrays in (b) and (c) is 100 nm. The particle-based nanolines, thus, have an interparticle gap, as well as a periodic gap between the line structures. The insets show the spectra of the structures in air.

developed by Sannomiya *et al* [19]. Controlled nano-object chemical growth in combination with LSPR could be such a technique for the conscious adaptation of pre-existing gold nanostructures directly on the nanoscale.

This work demonstrates how LSPR can be used to monitor the *in situ* growth of gold nano-objects and nanostructures. By exposing highly ordered gold nanoparticles and parallel arrays of evaporated gold nanowires to a commercial gold enhancement solution and optically tracking changes in the extinction spectrum it becomes possible to further adapt and tailor these pre-existing gold structures. This is useful to achieve more desirable physical dimensions, optical or electrical properties. This is attained e.g. when line-patterned nanoparticles grow into each other to create a conductive path and/or when the gap separating parallel nanowires shrinks, resulting in an enhanced resonance field or even a coupling of fields. Thus, the term 'gold enhancement' seems to be appropriate to describe not only the growth of gold, but also the intended improvement of the gold nanowire arrays, in this case for the purpose of using the improved arrays for (bio-)electrochemical sensing applications.

The presented *in situ* technique makes the dynamic growth of nano-objects visible and, thus, controllable without the necessity of characterizing the growth and aggregation kinetics of the gold enhancement solution. For the interested reader, the growth of colloidal gold has been studied with such techniques as electron microscopy and absorption spectroscopy by Seshadri *et al* [21]. Becker *et al* used a fast single-particle spectroscopy (fastSPS) method to observe and quantify the *in situ* growth of single nanoparticles [3]. The aggregation kinetics of colloidal gold has been investigated by measuring the polarized relaxation time by Wilcoxon *et al* [27]. Perhaps the most critical physical parameter of the presented nanosystems is the gap size (e.g. interparticle separation) and its influence on the plasmonic properties during gold growth. Fortunately, the influence of gap size on the optical response of nanoparticles has been widely studied [1, 5, 16]. The particle pairs, studied at various separation distances, at the point of touching and at various degrees of overlapping, correspond well to the various stages of gold growth in this work.

Densely packed hexagonal gold nanoparticle films, gold particle-based nanolines and evaporated gold nanowires are the three systems that have been investigated in this work. For a given particle size, nanoparticle films are interesting for their relatively homogeneous interparticle gaps. Particle-based nanolines consist not only of the same interparticle gaps, but due to the periodicity of the nanoline array there exists an interlinear gap. A controlled growth of such structures would result in a transformation of the line array into a conductive wire array as the particles grow into each other and eliminate the interparticle gap, while still maintaining an interlinear gap. The term 'nanowire' is reserved for conductive nanolines.

Experiments were designed to observe the overgrowth of these three systems with the intention of studying the observed changes in the peak position, peak height (i.e. extinction intensity) and peak width (e.g. radius of curvature) of the LSPR spectrum over time. These parameters were examined both experimentally and by simulation. Ultimately sufficient understanding of the growth kinetics could be obtained to controllably and repeatedly transform particle-based nanolines into a denser, wider and better defined nanowire structure with improved optical and electrical properties.

2. Materials and methods

The three nanosystems: hexagonally arranged gold nanoparticle monolayers, gold particle-based nanolines and evaporated gold nanowires are shown in figure 1 with their corresponding spectra. The nanoparticle monolayers were made by particle self-assembly [4]. For the first sample of hexagonally arranged gold nanoparticles, a concentrated suspension of 50 nm gold colloid particles (British Biocell) was deposited on a plasma-cleaned glass substrate. With a slight tilt of the substrate, the suspension on the glass was dried slowly, letting the colloidal particles assemble in a hexagonal arrangement with close packing at the descending liquid edge by capillary force.

For the two other types of samples the nanoline arrays in is this work were created using extreme ultraviolet light interference lithography (EUV-IL) exposed PMMA resist according to already published protocols based on the molecular assembly patterning by lift-off (MAPL) process [6, 22]. Niobium oxide (Nb_2O_5)-coated glass wafers with the PMMA pattern were used as the substrate for all fabricated nanowire arrays. For nanoparticle line patterns, an oxygen plasma treatment of 5 s was used to render a negative surface charge to the Nb_2O_5. A positively

charged polyethyleneimine (PEI) was then used to adhere the negatively charged DNA-coated gold particles to the substrate [22, 23]. The final lift-off in acetone and water resulted in clearly defined particle lines that were not dense enough for electrical conduction [12, 14]. The width of the lines is determined by lithography, but the height of the nanowire depends mainly on the size of the nanoparticles and the duration of subsequent gold enhancement. Except for the creation of the EUV-IL nanolines this bottom-up, self-assembly approach does not require cleanroom conditions, vacuum, or extensive cleaning. The resulting electrical properties differ from the continuous nanowires, but the additional surface area could prove more advantageous and sensitive to surface interactions. Additionally, there exists the possibility to embed other particles or nano-objects (e.g. carbon nanotubes) into the nanowire structure, thus further tailoring the optical or electrical properties.

For the evaporated gold nanowires, chromium was initially evaporated at a tilted angle of 15°. This forms a mushroom-like structure on top of the PMMA lines that prevents the subsequent deposited metal at normal incidence from covering substrate near the PMMA walls. Then 15 nm gold was evaporated at normal incident angle at a rate of 1 nm s^{-1} and a pressure of 2×10^{-6} mbar. The resulting line width of the gold wires is smaller than the gaps between the PMMA lines due to the shadowing effect of the mushroom-like chromium structure. This under-cut profile is necessary for the final PMMA lift-off. The nanowire quality mainly depends on the resist pattern roughness, the properties of the metal and the conditions for metal deposition.

Gold ions in solution are catalytically deposited onto the gold nanoparticles as metallic gold (Au_0) with the commercial solution GoldEnhance EM (Nanoprobes, USA). The nanoparticles or gold surface grow in size with development time. The solution is known to have a low level of autonucleation and at its recommended mixing concentration the growth of the nanoparticles and nanowires is readily measurable over minutes by monitoring the extinction spectra. The refractive index of the solution was measured to be 1.333 61 with a J357 automatic refractometer (Rudolph Research Analytical, US). The baseline formation of all measurements, the rinsing, and solution dilutions were performed with ultrapure water (18.2 MΩ cm @25 °C, Milli-*Q*, Millipore Corporation, Switzerland).

In this work all LSPR results have been collected with transmitted light through the sample, thus permitting the observation of the extinction spectrum peak and intensity. All samples for *in situ* experiments were built into custom-made flow cells with PDMS sealing rings (see supporting data available at stacks.iop.org/Nano/22/055203/mmedia). The spectra were recorded by a SpectraPro 2150 (PIXIS 400, Princeton Instruments, USA) using halogen lamp illumination with no polarization. The recorded information was evaluated by a custom-made program. The peak position, peak height (i.e. extinction intensity), and spectral width (e.g. radius of curvature) were determined by fitting the spectrum with a parabolic function.

For simulations the calculation of the extinction spectra was performed with the multiple multipole program (MMP) using the MaX-1 software package [9]. Spherical particles in a hexagonal arrangement and cross-sections with nanowire dimensions were modelled. For isolated spherical particles, the MMP gives an accuracy of more than ten digits as the MMP approach is based on analytical Mie scattering theory [9]. The dielectric constant of water was assumed to be non-dispersive at 1.777. The measured data of Johnson *et al* were used to determine the dielectric constant of gold [10]. For SEM imaging, the samples were coated with carbon for hexagonally arranged particles or platinum for the wire structures.

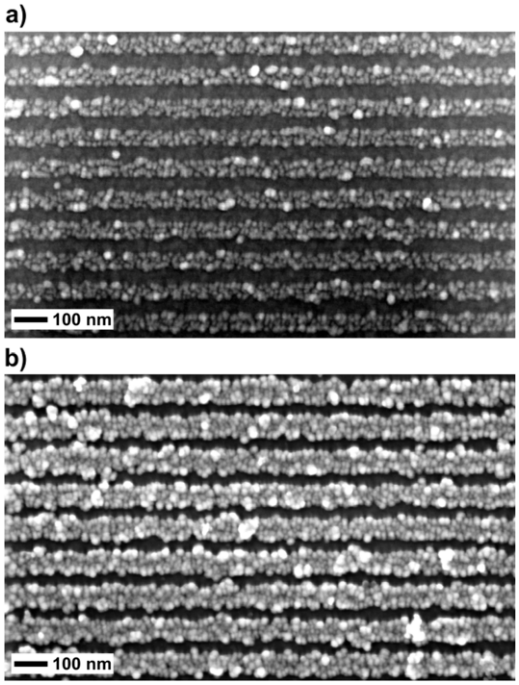

Figure 2. An example of the non-LSPR, time-based enhancement method, which only occasionally resulted in the successful transformation of (a) particle-based nanolines into (b) well-formed nanowires. In the SEM images are nanolines with a 100 nm period and originally formed with 5 nm gold nanoparticles.

3. Results and discussion

As a counter example to *in situ* control, gold nanowire enhancement can be performed without a flow cell by simply coating the surface of the sample substrate with the enhancement solution. As the scattering properties of the surface structures change, the enhancement of the nanolines is visible with the eye. In this way the enhancement of multiple particle-based nanoline samples for different lengths of times occasionally resulted in well-formed, conductive nanowires, as shown in figure 2. However, this method of time-based enhancement has proven to be neither reliable nor successfully repeatable. One can, therefore, not speak of control. Even before attempting to enhance the wires the exact initial dimensions of the wires are often unknown, because SEM imaging requires coating of the non-conductive substrate, thus rendering the sample unusable. Furthermore, the potencies of the enhancement solutions slightly differ with

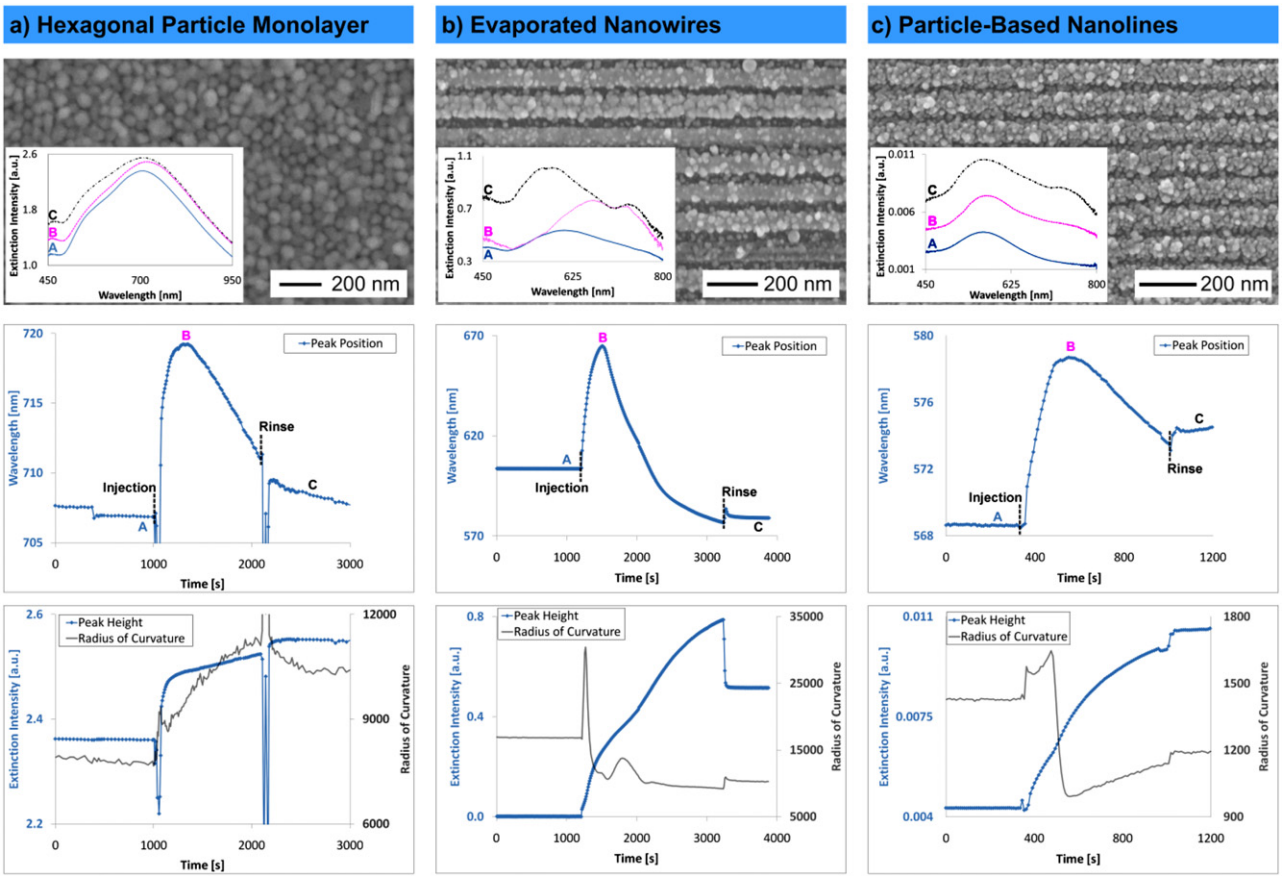

Figure 3. The corresponding post-enhanced nanosystems to those in figure 1 are displayed in an SEM image with their growth kinetics underneath: peak position, peak height and radius of curvature as a function of time. The spectra before injection, at maximum and after rinsing are inserted in the SEM images: (a) the hexagonally arranged nanoparticles; (b) the evaporated gold nanowires; (c) the particle-based nanowires. From the SEM images (b) and (c) it seems that autonucleation may have occurred due to the extended exposure time for evaporated and particle-based nanowires. This could explain the many small particles between the wires where no gold was earlier present.

age or batch. Thus, the result is often either an under-grown (i.e. non-conductive) or an over-grown (i.e. film-like) nanoline structure. By tracking the optical scattering and absorption (i.e. extinction) response during the enhancement process it was possible to both observe and eventually control the growth of the nanostructures.

3.1. In situ gold enhancement

Now, using a flow cell, the three nanosystems were exposed to the enhancement solution and observed from their original state to beyond the formation of interconnections as the individual nanostructures grew into each other. The resulting extinction spectra yielded valuable information and observations as particles grew into neighbouring particles and lines grew into neighbouring lines. An additional intention was the attempt to identify features of the extinction spectrum in the growth kinetics (i.e. peak position, height and width), which would enable an *in situ* control of the system's growth; for example, the identification of the phase where the nanoparticles in the particle-based nanolines have grown into one another, thus having become conductive, while still having preserved a gap between neighbouring nanowires.

Figure 3 provides a comprehensive summary of the resulting nanosystems after enhancement and their corresponding growth kinetics. All three nanosystems initially show an increase of the LSPR peak wavelength to a maximum after several minutes of growth, followed by a steady decline in the wavelength until the flow cell is rinsed. The rate of this growth and the time until the growth maximum is reached depend on the amount of gold, as well as on the gaps between the nanostructures (both interparticle or interlinear, as applicable). The concentration of the enhancement solution also plays a role. For the hexagonally arranged 50 nm gold nanoparticles the enhancement solution was 50% diluted with water. Otherwise, due to the amount of gold on the surface, the growth would be too rapid to capture with a reasonable sampling resolution. The nanoline and nanowire systems were enhanced with non-diluted and equally mixed enhancement solutions. As can be seen in the inset images of figure 3, double-peaks occasionally begin to form in the spectrum with continued growth. When the spectrum is understood as a superposition of LSPR frequencies, a newly formed peak is a representation of a newly excited mode. This occurs when new gold growth begins to change the original surface roughness of the structures (i.e. nanowires) and/or new features are created on their surfaces.

The hexagonal monolayer of nanoparticles would grow into a type of film at or just after the maximum since it lacks

the interlinear gap of the nanoline system. The interparticle gap is only a few nanometres (<5 nm), except for the packing defects due to different sizes, as well as 'dislocations' and 'vacancies'. According to figure 3(a) the time needed to reach maximum was 300 s with a recorded change in peak position of 13 nm. This roughly corresponds to a peak position change of 2.6 nm min^{-1} $[\Delta\lambda/\Delta t]$. According to the previous reports, the peak position stops red-shifting and turns to blue-shift as soon as coupled particles are connected [1, 5, 16]. Although particle growth in this system is not as homogeneous as simulations and involves other phenomena, such as nucleation of small particles, a similar coupling effect partially played a role for the red- and blue-shifting of the peak.

The evaporated nanowire system had no interparticle gaps. The nanowires were roughly 55 nm wide and 15 nm high. The distance between the nanowires was, therefore, roughly 45 nm. With consequently less gold (i.e. less surface coverage and smaller particle sizes) than the previous hexagonal monolayer of nanoparticles and in a non-diluted enhancement solution, the maximum was reached roughly 300 s after injection. In this time the peak position wavelength shifted 61 nm, which corresponds to a peak position change of 12.2 nm min^{-1} $[\Delta\lambda/\Delta t]$. As is evident from the SEM image in figure 3(b), although the lines themselves are wider, the interlinear gaps are not completely closed. The lines are irregularly interconnected at many locations along the wires. Note that the exposure to the enhancement solution results in a particle-like growth on the nanowire surface. The sharp topographical features on the nanowire's surface probably influence some form of preferential catalytic growth. However, further investigation is necessary to offer a conclusive reason.

The original particle-based nanoline system had both interparticle and interlinear gaps. The nanolines were roughly 90 nm wide and 5 nm high, due to 5 nm gold nanoparticles. Thus, the interlinear gap was extremely small in this sample, measuring roughly 10 nm. The growth phase in non-diluted enhancement solution is shorter and the shift in peak position wavelength is much smaller than for the evaporated nanowires. The growth maximum was reached in approximately 210 s, during which the peak position wavelength shifted 10 nm. This corresponds to a peak position change of 2.9 nm min^{-1} $[\Delta\lambda/\Delta t]$.

The rapid increase in the wavelength (red-shift) of the peak position upon exposure to the enhancement solution is obviously the effect from the gold growth. As the curve approaches a maximum, the nanogaps of the systems play an important role. In a particle-based nanoline system the interplay between the nanoparticle gaps and the interlinear gaps is also relevant. On a complete system level it is hypothesized that the maximum LSPR peak wavelength during growth corresponds to the moment at which a vast majority of interparticle gaps are closing and all particles or lines grow into each other at various positions along the length of the lines. Observations show that the lines do not grow perfectly homogeneously along their length, and thus do not contact each other at the same moment during growth. This suggests that the LSPR wavelength maximum arises from a delicate balancing act between simultaneous moments of contact (i.e. resonance shifts to higher wavelengths) and overgrowth (i.e. resonance shifts to lower wavelengths) at multiple points along the line structure. Therefore, to ensure that lines do not grow into each other, it would be necessary to stop the growth reaction before the maximum is reached.

These observations correspond well to the theoretically and experimentally observed optical response of nanoparticle systems. Theoretically, at the moment when two objects touch each other a singularity of the field at the touching point is created, as well as in the spectrum shifting the resonance infinitely to higher wavelengths for plasmonic objects. As soon as a neck is formed between the objects, the resonance shifts back to blue and keeps blue-shifting as the neck grows [1, 5, 16]. Although this is not strictly the case in real metals, the general behaviour of strong red-shifting followed by blue-shifting upon touching remains the same.

A continuous increase of the extinction intensity can be observed as more and more gold is present over time. This increase in intensity continues until the water rinse, at which point all parameters (i.e. peak position and peak height) display artefacts as a result of the solution exchange. The change in the spectral width, here shown as the radius of curvature, is also of interest. In all three cases the radius of curvature displays a radical change upon injection of the enhancement solution. It is possible that a type of chaotic growth is initiated as the catalytically released gold comes into contact with the pre-existing gold [15]. Based on the original geometry and the type of system order, such as a line pattern, a complex activation of resonance modes may occur and result in a broadening of the peak until the growth reaction stabilizes. Only in the case of the hexagonally arranged particle layer does the radius of curvature then continue to increase. In the nanoline and nanowire systems the initial change upon injection is followed by a steady sharpening of the spectrum until some minimum of the radius of curvature is reached. This minimum corresponds almost exactly to the maximum of the LSPR peak wavelength. A reliable calculation of the radius of curvature can be difficult if the shape of the spectrum becomes too complex. Therefore, concrete conclusions with this parameter should be avoided until a larger body of data can be obtained.

3.2. Simulation

To better understand the plasmonic properties associated with gold growth, simulations with MMP were performed for the hexagonal nanoparticle system and the evaporated gold system. The LSPR spectrum was analysed at two main stages of growth: at the original system dimensions and shortly before the nanostructures grew into each other (i.e. small gap sizes). The evaporated gold nanowires were additionally simulated at a stage of over-enhancement at the point where the structures slightly grew into each other, as seen in figure 4. An example of the field pattern from the simulation of the hexagonally arranged nanoparticles can be found in the supporting data (available at stacks.iop.org/Nano/22/055203/mmedia).

By simulating the spectral response it was possible to study and to compare the effect of gold growth on the peak position and peak height with the experimental

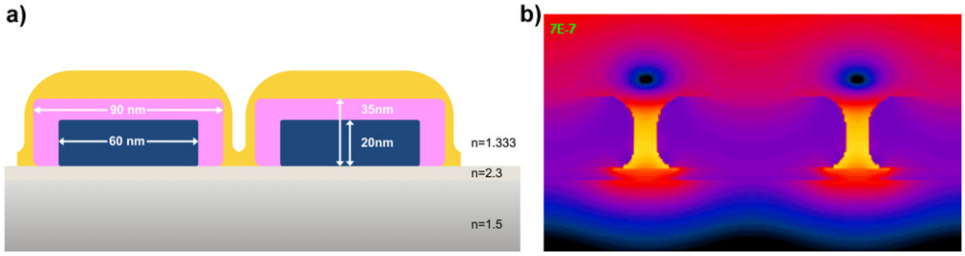

Figure 4. (a) A cross-sectional illustration of the geometries used to simulate the growth of the nanowires at the original dimension (blue), after 15 nm homogeneous growth (pink) and after having slightly grown together (yellow). These colours correspond to the colours of the simulated spectra. (b) A time averaged electric field distribution of the nanowires after 15 nm growth at peak resonance ($\lambda = 700$ nm).

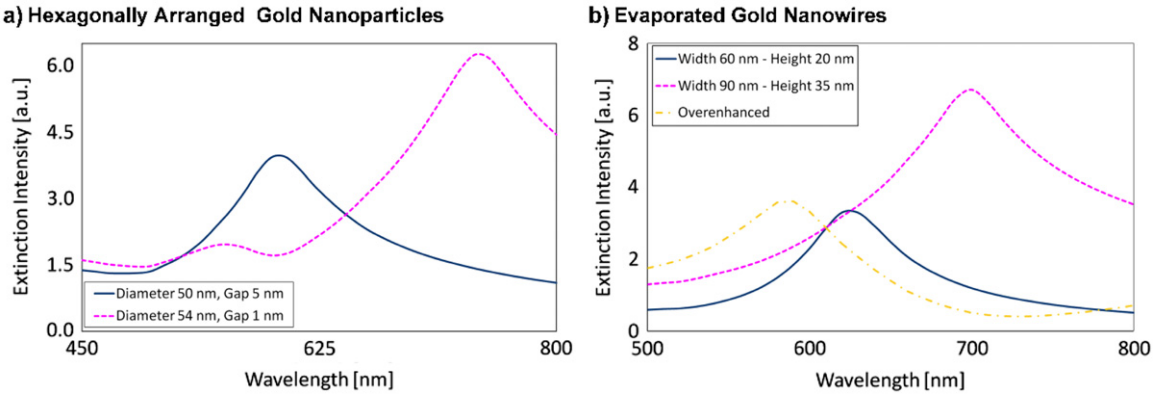

Figure 5. The simulated extinction spectra at different stages of gold growth of the (a) hexagonally arranged gold nanoparticles and (b) evaporated gold nanowires. Both systems experience a shift to higher wavelengths (red-shift) during the initial growth phase. The simulated over-enhancement of the nanowires results in a shift to lower wavelengths (blue-shift), which is consistent with the experimental results.

results. Figure 5 shows the simulated results from the hexagonally arranged gold nanoparticles and the evaporated gold nanowires.

The peak positions of the simulated extinction spectra behave similarly to the experimentally obtained spectra, as seen in figures 5(a) and (b). An initial positive shift to higher wavelengths (red-shift) is observed as the gap sizes decrease. A simulated over-enhancement of the evaporated gold nanowires also results in a strong negative shift to lower wavelengths (blue-shift). The simulation does not present the exact moment of contact when a singularity of the field is expected to be created and as the spectrum shifts the resonance to infinity, before again decreasing as the overgrowth continues [1, 5, 16].

From the simulation the extinction response only partially corresponded to the experimental results. Despite an initial increase in intensity upon growth, a simulated over-enhancement yielded a decrease in the intensity. The experimental results show a steady increase in intensity until rinsing, which is intuitively the expected response. This underscores some limitations of the simulation. Firstly, no differentiation is made between the pre-existing gold and the additional crystal structure of the chemically grown gold. Therefore, the roughness of the structures cannot be easily simulated and features such as double-peaks in the spectrum are not visible. Secondly, the simulated cross-section of the evaporated gold nanowires is a simplification of the actual structure. As is evident from the SEM images of figure 3(b), there are points along the wire at which the nanowires have grown together, but also points where gaps still exist. The discontinuity of the cross-section along the wires (i.e. an additional length dimension) is more demanding to simulate.

3.3. Controlled in situ gold enhancement

Based on the information obtained from the experimental and simulated results, the controlled growth of particle-based nanowires was attempted. A particle-based nanoline sample was prepared from an EUV-IL developed substrate with nanolines of 200 nm periodicity. Such samples have wider lines, but consequently also larger interlinear gaps (e.g. ∼50 nm), while the interparticle gaps remain the same as in the previous particle-based systems (e.g. ∼5 nm). This extra room to grow makes it easier to separate the touching moment of interparticle gaps from that of interlinear gaps, since they no longer share the same order of dimension. In other words, although the particles grow at the same rate as previous experiments with lines of 100 nm periods, the particles grow into each other to form continuous lines/wires long before the adjacent lines grow into each other.

Again 5 nm gold nanoparticles were attached to the substrate with the same fabrication method as presented above. Due both to the small particle size and the large interlinear gaps the scattering effect is so small that the

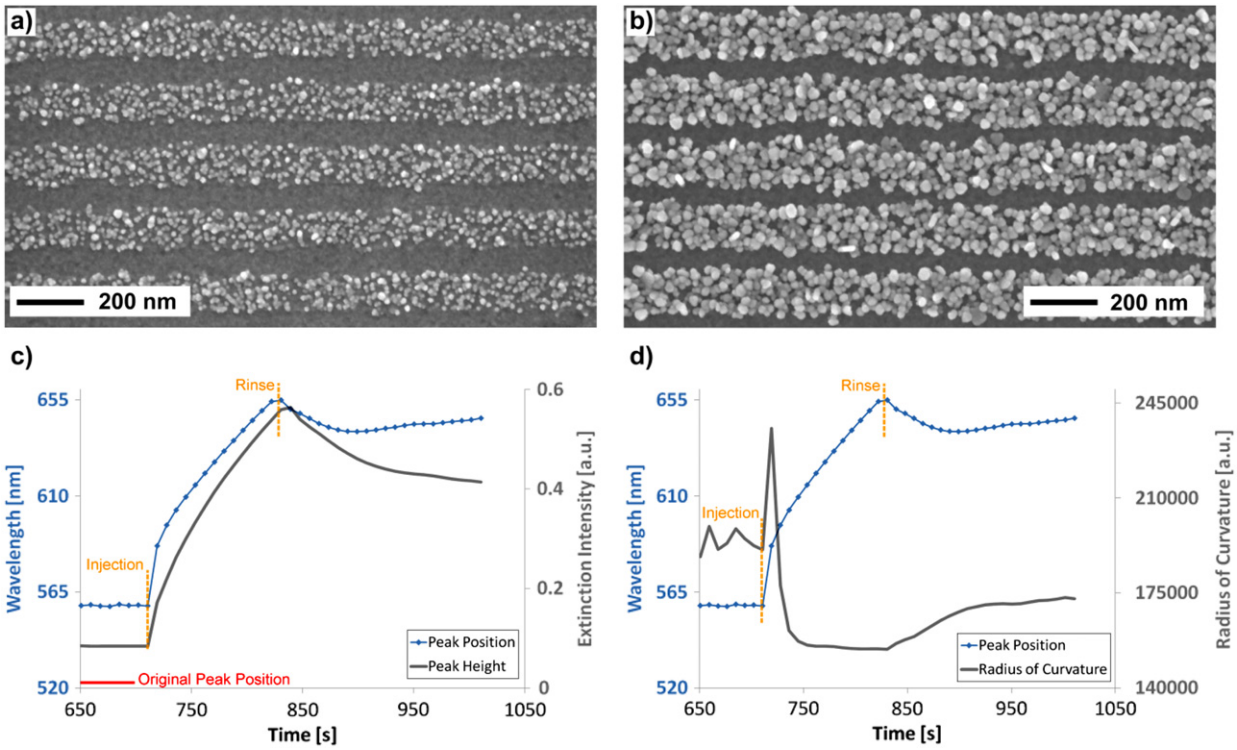

Figure 6. The SEM images of the particle-based nanowire sample at the stateS of (a) 20 s of pre-enhancement and (b) after *in situ* enhancement and rinsing in the flow cell. The plots (c) and (d) summarize the growth kinetics as a function of peak position, peak height and peak width. The original LSPR peak wavelength of the unenhanced nanolines is marked in (c). The spectra of the nanolines and their corresponding SEM images can be found in the supporting data (available at stacks.iop.org/Nano/22/055203/mmedia).

structures are barely visible by eye or even under the light microscope of the spectrometer. To increase the visibility of the nanolines for proper measurement alignment they were enhanced outside of the flow cell for 20 s prior to their recorded *in situ* measurement. More information about the original nanoline spectrum can be found in the supporting data (available at stacks.iop.org/Nano/22/055203/mmedia). The sample was exposed to the enhancement solution, but the reaction was interrupted with a water rinse before the LSPR peak wavelength reached a maximum and while the radius of curvature continued to decline before reaching a minimum. Figure 6 summarizes the results.

As is apparent from the SEM images, the particle-based nanoline system in figure 6(a) is transformed into wider, yet well-formed nanolines with an obvious change in the individual particle size, figure 6(b). Analogous to the measurements from figure 3 there is an initial rapid increase in all three monitored parameters (peak position, peak height and radius of curvature). In all nanoline experiments so far the rapid increase in the radius of curvature is followed by a sharpening of the peak as indicated by the decreasing radius of curvature. Due to the pre-enhancement of the nanolines the growth phase may appear to be slightly shorter than other measurements, but the growth would have begun at the original LSPR peak wavelength, as indicated in figure 6. In total, enhancement took place for 140 s (including 20 s of pre-enhancement). In this time the peak position wavelength shifted 130 nm, which corresponds to a peak position change of 55.7 nm min^{-1} $[\Delta\lambda/\Delta t]$.

For this particular experiment the conductance of the resulting nanowires was not tested due to a lack of metal contacts, which could have influenced the gold enhancement. Conductance of particle-based nanowires has, however, been confirmed with four-terminal sensing by establishing a connection to the nanowire arrays with silver paste [22]. In addition, the enhancement of the nanolines was successfully controlled to create a nanoline system with increased extinction intensity, a larger LSPR peak wavelength and a sharper, better defined peak. The spectra can be found in the supporting data (available at stacks.iop.org/Nano/22/055203/mmedia).

4. Conclusions and outlook

This work demonstrated how LSPR can be used to monitor the *in situ* growth of gold nano-objects and nanostructures for their controlled modification. This could prove to be a valuable method to enhance the plasmonic properties and electrical conduction of gold and perhaps silver nanosystems. Although the plasmonic properties were tracked as a function of LSPR peak wavelength, extinction intensity and spectral width, the LSPR peak wavelength (also referred to as peak position) was shown to be the critical parameter. No stable conclusions could be drawn from the spectral width, measured as the peak radius of curvature. Finally it was shown that a particle-based nanoline array could be controllably grown into a conductive nanowire array. Despite the strong experimental support that the maximum in the *in situ* measured peak position

is a critical moment in the growth process, the exact optimal moment to interrupt the gold enhancement has still not been identified. Nevertheless, the newly obtained consistency in the fabrication of particle-based nanowires will allow for their reliable electrical characterization. Work is already underway to integrate the particle-based nanowire arrays into a microfabricated chip for electrical inspection. In the near future, protected metal contacts of materials other than gold will also be connected to the nanowire arrays to attempt an *in situ* electrical measurement as the particle-based nanolines grow into conductive nanowires.

The development and improvement of this method could impact such fields as nanogap sensing, biosensing and nanoelectronics. For example, in the future it could be possible to combine this type of enhancement with gold nanoparticles that have been synthesized on SiO_2 nanowires as a step toward combining plasmonics with semiconductor nanowire technology [11]. The combined top-down and bottom-up fabrication method of the particle-based nanowires also allows the possibility of embedding other nano-objects, such as carbon nanotubes, quantum dots, or other nanoparticles into the linear arrangement of gold nanoparticles. A subsequent enhancement could then result in an interconnection of these nano-objects to form new types of highly ordered hybrid nanostructures with specific electrical and optical properties. This could include the embedding of e.g. proteins into grown gold or silver as a novel method of surface functionalization. In evaporated nanowire arrays where the electrical conductivity is already established, gold enhancement or particle growth could be used to optimize the LSPR response as the interlinear gap is reduced and the chance of LSPR field coupling increases. Furthermore, through additional growth the resistance of the nanowires and of the array could be adjusted and non-conducting wires could even be repaired.

Acknowledgments

We acknowledge and appreciate the generous financial support of this project from CCMX and from the Nano-Tera Initiative. In addition we wish to thank the Swiss Federal Institution of Technology (ETH Zürich), as well as the associated project partners at the Paul Scherrer Institute (PSI) with special mention to Dr Vaida Auzelyte.

References

[1] Atay T, Song J-H and Nurmikko A V 2004 Strongly interacting plasmon nanoparticle pairs: from dipole–dipole interaction to conductively coupled regime *Nano Lett.* **4** 1627–31

[2] Auzelyte V *et al* 2009 Extreme ultraviolet interference lithography at the Paul Scherrer Institut *J. Micro-Nanolithogr. MEMS MOEMS* **8** 10

[3] Becker J, Schubert O and Sönnichsen C 2007 Gold nanoparticle growth monitored *in situ* using a novel fast optical single-particle spectroscopy method *Nano Lett.* **7** 1664–9

[4] Blättler T M, Binkert A, Zimmermann M, Textor M, Vörös J and Reimhult E 2008 From particle self-assembly to functionalized sub-micron protein patterns *Nanotechnology* **19** 075301

[5] Danckwerts M and Novotny L 2007 Optical frequency mixing at coupled gold nanoparticles *Phys. Rev. Lett.* **98** 026104

[6] Falconnet D, Koenig A, Assi T and Textor M 2004 A combined photolithographic and molecular-assembly approach to produce functional micropatterns for applications in the biosciences *Adv. Funct. Mater.* **14** 749–56

[7] Ginger D S, Zhang H and Mirkin C A 2004 The evolution of dip-pen nanolithography *Angew. Chem. Int. Edn* **43** 30–45

[8] Groves T R, Pickard D, Rafferty B, Crosland N, Adam D and Schubert G 2002 Maskless electron beam lithography: prospects, progress, and challenges *Microelectron. Eng.* **61/2** 285–93

[9] Hafner C 2007 Boundary methods for optical nano structures *Phys. Status Solidi* b **244** 3435–47

[10] Johnson P B and Christy R W 1972 Optical constants of the noble metals *Phys. Rev.* B **6** 4370

[11] LaLonde A D, Norton M G, Zhang D Q, Gangadean D, Alkhateeb A, Padmanabhan R and McIlroy D N 2005 Controlled growth of gold nanoparticles on silica nanowires *J. Mater. Res.* **20** 3021–7

[12] MacKenzie R, Auzelyte V, Olliges S, Spolenak R, Solak H and Vörös J 2009 *Nanosystems Design and Technology* ed J Vörös *et al* (Heidelberg: Springer) pp 143–73

[13] MacKenzie R, Fraschina C, Dielacher B, Sannomiya T, Dahlin A and Vörös J 2010 Simultaneous measurement of the electrical and plasmonic properties of metal nanowire arrays upon potential induced ion binding *ACS Nano* submitted

[14] MacKenzie R, Fraschina C, Sannomiya T, Auzelyte V and Vörös J 2010 Optical sensing with simultaneous electrochemical control in metal nanowire arrays *Sensors* **10** 9808–30

[15] Polte J, Erler R, Thünemann A F, Sokolov S, Ahner T T, Rademann K, Emmerling F and Kraehnert R 2010 Nucleation and growth of gold nanoparticles studied via *in situ* small angle x-ray scattering at millisecond time resolution *ACS Nano* **4** 1076–82

[16] Romero I, Aizpurua J, Bryant G W and García De Abajo F J 2006 Plasmons in nearly touching metallic nanoparticles: singular response in the limit of touching dimers *Opt. Express* **14** 9988–99

[17] Sannomiya T, Dermutz H, Hafner C, Vörös J and Dahlin A B 2009 Electrochemistry on a localized surface plasmon resonance sensor *Langmuir* **26** 7619–26

[18] Sannomiya T, Hafner C and Vörös J 2008 *In situ* sensing of single binding events by localized surface plasmon resonance *Nano Lett.* **8** 3450–5

[19] Sannomiya T, Hafner C and Vörös J 2009 Strain mapping with optically coupled plasmonic particles embedded in a flexible substrate *Opt. Lett.* **34** 2009–11

[20] Sepúlveda B, Angelomé P C, Lechuga L M and Liz-Marzán L M 2009 LSPR-based nanobiosensors *Nano Today* **4** 244–51

[21] Seshadri R, Subbanna G N, Vijayakrishnan V, Kulkarni G U, Ananthakrishna G and Rao C N R 1995 Growth of nanometric gold particles in solution-phase *J. Phys. Chem.* **99** 5639–44

[22] Stadler B, Solak H H, Frerker S, Bonroy K, Frederix F, Vörös J and Grandin H M 2007 Nanopatterning of gold colloids for label-free biosensing *Nanotechnology* **18** 6

[23] Storhoff J J, Elghanian R, Mucic R C, Mirkin C A and Letsinger R L 1998 One-pot colorimetric differentiation of polynucleotides with single base imperfections using gold nanoparticle probes *J. Am. Chem. Soc.* **120** 1959–64

[24] Tseng A A 2005 Recent developments in nanofabrication using focused ion beams *Small* **1** 924–39

[25] Tseng A A, Chen K, Chen C D and Ma K J 2003 Electron beam lithography in nanoscale fabrication: recent development *IEEE Trans. Electron. Packag. Manuf.* **26** 141–9

[26] Tseng A A, Notargiacomo A and Chen T P 2005 Nanofabrication by scanning probe microscope lithography: a review *J. Vac. Sci. Technol.* B **23** 877–94

[27] Wilcoxon J P, Martin J E and Schaefer D W 1989 Aggregation in colloidal gold *Phys. Rev.* A **39** 2675–88